Solid State Communications, Vol. 87, No. 6, pp. 531-533, 1993.
Printed in Great Britain.

0038-1098/93$6.00+.00
Pergamon Press Ltd

PHASE STRAIN MODEL FOR CHARGE DENSITY WAVE SUB-DOMAIN FORMATION IN AN APPLIED TEMPERATURE GRADIENT

P. A. Parilla,* M. F. Hundley,** and A. Zettl

Department of Physics, University of California at Berkeley, Berkeley, CA 94720

(Received 29 April 1993 by A. Zawadowski)

The dynamics of a sliding charge density wave (CDW) condensate subjected to a uniform temperature gradient are examined within an elastic medium model. As the temperature gradient is increased, it becomes energetically favorable for the CDW to break up into a series of velocity sub-domains of equal size separated by phase slip centers. The number of sub-domains scales with the temperature gradient and with the length of the CDW crystal. Unusual dynamical asymmetries are also predicted depending on the relative direction of heat and current flow through the CDW crystal.

One of the most intriguing aspects of the collective mode charge density wave (CDW) state[1] is that it exhibits long-range phase coherence. For a dynamic (that is, "sliding") CDW condensate, the phase velocity coherence length is a macroscopic quantity. In materials such as $NbSe_3$, TaS_3, and $K_{0.3}MoO_3$, the characteristic parameters dictating the CDW response (such as normal-carrier damping, number of carriers in the CDW state, threshold electric field E_T, etc.) are, in general, very temperature dependent. Hence, for a given external drive condition (electric field or current), the CDW response (namely, the CDW drift velocity v_0) is temperature dependent.

For a sliding CDW crystal subject to a temperature gradient along the crystal axis, there exists a competition between the tendency for macroscopic CDW phase velocity coherence and the tendency for the CDW velocity to assume a distribution of values dictated by local conditions. Indeed, early narrow-band "noise" (NBN) experiments (where the well-defined noise frequency f_{NBN} gives[2] directly v_0) on $NbSe_3$ samples subjected to a temperature gradient have shown that for very short crystals, v_0 is single valued and reflects only the average sample temperature[3] while, for longer samples, the single velocity "domain" (apparent under isothermal conditions) breaks into two or more "sub-domains" with independent v_0's.[4,5] Thus, under appropriate conditions, an applied temperature gradient is able to break the CDW coherence and induce sub-domain formation.

In this report, we examine within a simplified model the competition between macroscopic phase velocity coherence and velocity sub-domain formation in a CDW crystal with an applied uniform temperature gradient. We model the CDW as an elastic medium[6-8] subject to internal temperature-gradient-induced strain where excessive strain is relieved by the formation of velocity sub-domains separated by phase slip centers (PSC). From a general energy minimization scheme, we find that in the high field limit ($E \gg E_T$) the sub-domains are of equal size and that the number of sub-domains N scales directly with the temperature difference ΔT across the sample and with the length L of the sample: $N \sim \Delta T^{2/3} L^{1/3}$ in one limit, and $N \sim \Delta T^{2/5} L^{3/5}$ in another limit. This prediction has, in part, been verified by recent experiments in $NbSe_3$.[9] In addition, for a given sub-domain, the model predicts asymmetries in v_0 with respect to the relative directions of heat and current flow through the crystal. This v_0 asymmetry may explain previously observed but poorly understood differences between noise spectra for positive and negative drive in CDW crystals.

We represent the charge density by the usual expression $\rho(x) = \rho_0 + \rho_1 \cos[Qx + \Phi(x,t)]$ where ρ_0 is the mean electronic charge density, ρ_1 is the density wave amplitude, $Q = 2k_F$ is the CDW wavevector, and $\Phi(x,t)$ is the position and time dependent CDW phase whose time derivative is related to the CDW velocity v_0. To conform with experimental observations, we assume that, with the application of a temperature difference ΔT across the crystal, the sample breaks into N sub-domains and that the CDW velocity v_0 is constant only over a particular sub-domain. Thus, for a given sub-domain, $\Phi(x,t) = Qv_0 t + \Phi(x)$ where $\Phi(x)$ is a (time independent) distortion. The coordinate $x = 0$ is here defined to lie in the center of the sub-domain.

Due to the temperature variation across the sub-domain, the moving CDW will generate a position-dependent internal elastic strain s which, in turn, leads to position dependences in the CDW wavevector, charge density, and damping. The internal strain is parameterized by $s = s(x) \equiv (1/Q)d\Phi(x)/dx = \Delta Q/Q$. Within a sub-domain, the CDW equation of motion is taken as[7]

$$\frac{\gamma(x)}{Q}\frac{d\Phi}{dt} - \frac{1}{Q}\frac{d}{dx}\left(\kappa(x)\frac{d\Phi}{dx}\right) = \rho_0(x)E(x) \qquad (1)$$

where γ and κ are, respectively, the CDW damping and elasticity. To first order, the position dependences of κ and the applied electric field E result from the temperature variation T(x) while the position dependence of ρ_0 is

*present address: Solar Energy Research Institute, 1617 Cole Boulevard, Golden, CO 80401, U.S.A.
**present address: Los Alamos National Laboratory, Los Alamos, NM 87545, U.S.A.

dominated by the strain $\rho_o(x) = \rho_o - \rho_s s$, and the damping has strain and temperature terms ($\gamma(x) = \gamma + \gamma'(\Delta T/L)x - \gamma_s s$). The high-field limit is assumed which eliminates the threshold field. In the limit of small ΔT, Eq. (1) leads to a sub-domain phase velocity

$$v_0 = \frac{\rho_o E}{\gamma}\left[\frac{1 - \frac{L_D E' \Delta T}{2EL}\xi\left(\frac{E}{\varepsilon}\right)}{1 - \frac{L_D \gamma' \Delta T}{2\gamma L}\xi\left(\frac{E}{\varepsilon}\right)}\right] \tag{2a}$$

$$\xi(v) = \coth(v) - \frac{1}{v} \tag{2b}$$

$$v \equiv \frac{E}{\varepsilon} \equiv \alpha\frac{L_D}{2} = \frac{\rho_s E L_D}{2\kappa}(1 - r)) \tag{2c}$$

where $\rho = (\rho_o\gamma_s)/(\gamma\rho_s)$ and the primes denote temperature derivates. The associated sub-domain strain s(x) derived from Eq. (1) is

$$s(x) = \frac{\left(\frac{\rho_0}{\rho_s}\right)\left(\frac{E'}{E} - \frac{\gamma'}{\gamma}\right)\frac{\Delta T}{L}\exp\left(-\frac{\kappa'\Delta T}{\kappa L}\right)}{(1 - r)\left\{1 - \frac{L_D\gamma'\Delta T}{2\gamma L}\xi\left(\frac{E}{\varepsilon}\right)\right\}} \times$$

$$\left[x + \frac{L_D}{2}\coth(v) - L_D\frac{\exp(\alpha x)}{\exp(v) - \exp(v)}\right] \tag{3}$$

where, again, the primes denote temperature derivatives. s(x) can be used to evaluate the phase strain energy U_s for the subdomain: $U_s = (1/2)\int \kappa(x)|s(x)|^2 dx$. Figure 1 shows the small ΔT-limit U_s plotted versus the domain length L_D for different values of the parameter α. Two regimes are evident. For small L_D (corresponding to the small-|v| limit), $U_s \sim (\Delta T/L))^2 L_D^3$ with no α dependence. The transition between the two scaling behaviors occurs at a length scale $\sim(1/\alpha)$. Physically in the small-|v| limit, the strain profile of the CDW is dominated by the normal restoring force of the CDW (as an elastic medium) while in the large-|v| limit the conversion between CDW/normal carriers dominates through ρ_s and γ_s.

The number and size of the sub-domains in the entire crystal is obtained by minimizing the total energy U_{tot} of the crystal. This energy involves a strain contribution U_{si} from each ith sub-domain, and a phase slip energy U_{ps} associated with each phase velocity discontinuity at sub-domain interfaces. An actual estimate for U_{ps} could be obtained by considering the PSC as a line of phase vortices which move transverse to the CDW axis where each vortex has an approximate energy proportional to $N(E_F)\Delta^2\xi_{\|}\xi_{\perp}$ where $N(E_F)$ is the density of states at the Fermi level, Δ is the CDW energy gap, and $\xi_{\|}$ and $\xi_{\perp}$ are, respectively, the CDW amplitude correlation lengths parallel and perpendicular to the chain axis.[5]

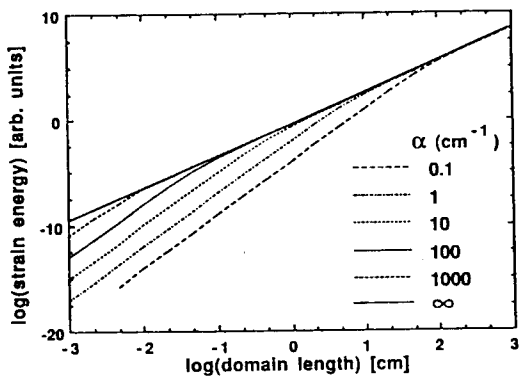

Fig. 1. Sub-domain strain energy U_S versus sub-domain size L_D calculated for various α. (See Eqs. (2a) and (3).)

Far from the transition temperature, these parameters are not very temperature dependent so we treat U_{ps} as being a constant independent of temperature and position.

For N sub-domains, the total energy becomes

$$U_{tot} = U_{ps}(N + 1) + U_{ts} \tag{4}$$

where we have defined the total strain energy $U_{ts} = \Sigma U_{si}$. The position of the sub-domain interfaces (which, in turn, dictates the individual sub-domain sizes L_{Di}) are found by minimizing, for a given N, the total strain energy U_{ts}. With p_i, the position of the ith phase slip interface, the appropriate minimization condition is[10] $\partial U_{ts}/\partial p_i = dU_s(L_{Di})/dL_D - dU_s(L_{Di+1})/dL_D = 0$, $1 \le i \le N - 1$, which has the solution $L_{Di} = L/N$, that is, all the sub-domains are of equal size. With this assignment, Eq. (4) leads to

$$U_{tot,N} = U_{ps}(N - 1) + \frac{B_m(\Delta T)^2 L^{m-2}}{N^{m-1}} \tag{5}$$

where B_m is a weak function (and can be taken as a constant) whose limiting form depends on |v|, and m = 3 in the large-|v| limit and m = 5 in the small-|v| limit. The second term on the right in Eq. (5) is $U_{ts} \equiv U_{sl}/N^{m-1}$. The critical value at ΔT at which the total number of sub-domains in the crystal will change by one is determined from Eq. (5) by setting $U_{tot,N} = U_{tot,N+1}$. This leads to

$$\frac{U_{sl}}{U_{ps}} = \frac{N^2(N + 1)^2}{2N + 1} \qquad (\text{large}\,|v|) \tag{6a}$$

$$\frac{U_{sl}}{U_{ps}} = \frac{N^4(N + 1)^4}{4N^3 = 6N^2 + 4N \pm 1} \qquad (\text{small}\,|v|) \tag{6b}$$

Figure 2 shows the total number of sub-domains N plotted versus the normalized strain energy U_{sl}/U_{ps}, appropriate to the large-|v| limit. In the limit of large N, the

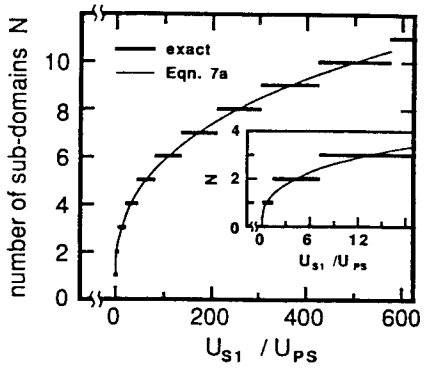

Fig. 2. Number of sub-domains N versus normalized strain energy U_{sl}/U_{ps} calculated in the large-|v| regime (Eq. (6a)). The approximate expression for N (Eq. (7a)) is also plotted for comparison (solid line). The inset shows in detail N for small strain energy.

number of sub-domains can be written in closed form:

$$N = \left(\frac{2U_{sl}}{U_{ps}}\right)^{1/3} = \left(\frac{2B_m[\Delta T]^2 L}{U_{ps}}\right)^{1/3} \quad \text{(large } |v|\text{)} \qquad (7a)$$

$$N = \left(\frac{4U_{sl}}{U_{ps}}\right)^{1/5} = \left(\frac{2B_m E^2[\Delta T]^2 L^3}{U_{ps}}\right)^{1/5} \quad \text{(small } |v|\text{)} \qquad (7b)$$

which demonstrates directly a surprising scaling between N and ΔT for fixed L and between N and L for fixed ΔT. The solid line in Fig. 2 is Eq. (7a) which compares favorably with the numerical solution even in the range of small N (see inset).

Recent experiments on $NbSe_3$ have carefully examined the relation between the sub-domian number N and the applied temperature gradient ΔT.[9] The relation $N \sim (\Delta T)^{2/3}$ is accurately obeyed for several $NbSe_3$ specimens over a wide range of ΔT for both positive and negative values of ΔT. This scaling behavior is consistent with Eq. (7a) and suggests that typical samples of this material fall into the large-|v| limit. For N = 4 or 5, the relative energy scale is $U_{sl}/U_{ps} \sim 50$. The scaling relation of N versus sample length L has not yet been tested.

We also note that Eq. (2), the expression for the CDW velocity v_o within a sub-domain, has an unusual asymmetry with respect to the signs of E and ΔT. If *both* ΔT and E are reversed, the equation remains invariant. On the other hand, if only ΔT or only E is reversed in sign, the expression for v_o is markedly different. The magnitude of v_o plays an essential role in determining N in Eq. (6). Hence, in the presence of a fixed-temperature gradient, the model suggests that a different number of sub-domains can result depending on the relative directions of the electrical and heat currents in the sample. This has been observed experimentally in $NbSe_3$.[9] Furthermore, this phenomenon may be the cause of asymmetries observed in the noise spectra of CDW conductors under *isothermal* conditions. In those cases, an inhomogeneous impurity distribution may manifest itself as (very loosely speaking) a "built-in" temperature gradient (that is, a built-in strain asymmetry) with the consequent difference in domain configuration or magnitude of v_o for positive and negative drive bias.

We thank Professor L. M. Falicov for encouragement and helpful interactions throughout the course of this study. This research was supported by NSF Grant DMR-9017254.

References

1. For a review, see G. Grüner and A. Zettl, Phys. Rep. **119**, 117 (1985); see also P. Monceau in *Electronic Properties of Quasi-One-Dimensional Materials*, Vol. II, ed. P. Monceau (Reidel, Dordrecht, 1985), p. 139.
2. P. Monceau, J. Richard, and M. Renard, Phys. Rev. Lett. **45**, 43 (1980).
3. A. Zettl, M. Kaiser, and G. Grüner, Solid State Comm. **53**, 649 (1985).
4. X.-J. Zhang and N. P. Ong, Phys. Rev. B **30**, 7343 (1984); M. F. Hundley and A. Zettl, Phys. Rev. B **33**, 2883 (1986); S. E. Brown, A. Janossy, and G. Grüner, Phys. Rev. B **31**, 6869 (1985); J. W. Lyding, J. S. Hubacek, G. Gammie, and R. F. Thorne, Phys. Rev. B **33**, 4341 (1986).
5. N. P. Ong, G. Verma, and K. Maki, Phys. Rev. Lett. **52**, 663 (1984); G. Verma and N. P. Ong, Phys. Rev. B **30**, 2928 (1984).
6. D. Feinberg and J. Friedel, J. de Phys. **49**, 485 (1988).
7. L. Sneddon, M. C. Cross, and D. S. Fisher, Phys. Rev. Lett. **49**, 292 (1982).
8. P. A. Parilla, M. F. Hundley, and A. Zettl, to be published.
9. P. A. Parilla, A. Behrooz, and A. Zettl, see companion paper *Solid State Commun.* **87**, 527 (1993).
10. Actually, U_{ts} is a more complicated function of the p_i than just the L_{Di} ($= p_i - p_{i-1}$) dependence; however, the L_{Di} dependence strongly dominates. (see Ref. 8)